Osteoprogenitor SFRP1 prevents exhaustion of hematopoietic stem cells via PP2A-PR72/130-mediated regulation of p300

Franziska Hettler,[1][*] Christina Schreck,[1][*] Sandra Romero Marquez,[1] Thomas Engleitner,[2,3] Baiba Vilne,[4,5] Theresa Landspersky,[1] Heike Weidner,[6] Renate Hausinger,[1] Ritu Mishra,[2,7] Rupert Oellinger,[2,3] Martina Rauner,[6] Ronald Naumann,[8] Christian Peschel,[1,9] Florian Bassermann,[1,9] Roland Rad,[2,3,9] Rouzanna Istvanffy[1°#] and Robert A.J. Oostendorp[1#]

[1]Technical University of Munich, School of Medicine, Department of Internal Medicine III Hematology/Oncology, Munich, Germany; [2]Technical University of Munich, School of Medicine, Center for Translational Cancer Research (TranslaTUM), Munich, Germany: [3]Technical University of Munich, School of Medicine, Institute of Molecular Oncology and Functional Genomics, Munich, Germany; [4]Bioinformatics Research Unit, Riga Stradins University Riga, Riga, Latvia; [5]netOmics, Riga, Latvia; [6]Bone Lab Dresden, Department of Medicine III & Center for Healthy Aging, Technische Universität Dresden, Dresden, Germany; [7]School of Medicine, Institute of Clinical Chemistry and Pathobiochemistry, Technical University of Munich, Munich, Germany; [8]Max Planck Institute of Molecular Cell Biology and Genetics, Transgenic Core Facility, Dresden, Germany and [9]German Cancer Consortium (DKTK), Heidelberg, Germany

°*Current affiliation: Technical University of Munich, School of Medicine, Surgery Department, Munich, Germany*

**FH and CS contributed equally as co-first authors.*
#RI and RAJO contributed equally as co-senior authors.

Abstract

Remodeling of the bone marrow microenvironment in chronic inflammation and in aging reduces hematopoietic stem cell (HSC) function. To assess the mechanisms of this functional decline of HSC and find strategies to counteract it, we established a model in which the *Sfrp1* gene was deleted in Osterix+ osteolineage cells (OS1$^{\Delta/\Delta}$ mice). HSC from these mice showed severely diminished repopulating activity with associated DNA damage, enriched expression of the reactive oxygen species pathway and reduced single-cell proliferation. Interestingly, not only was the protein level of Catenin beta-1 (β-catenin) elevated, but so was its association with the phosphorylated co-activator p300 in the nucleus. Since these two proteins play a key role in promotion of differentiation and senescence, we inhibited *in vivo* phosphorylation of p300 through PP2A-PR72/130 by administration of IQ-1 in OS1$^{\Delta/\Delta}$ mice. This treatment not only reduced the β-catenin/phospho-p300 association, but also decreased nuclear p300. More importantly, *in vivo* IQ-1 treatment fully restored HSC repopulating activity of the OS1$^{\Delta/\Delta}$ mice. Our findings show that the osteoprogenitor *Sfrp1* is essential for maintaining HSC function. Furthermore, pharmacological downregulation of the nuclear β-catenin/phospho-p300 association is a new strategy to restore poor HSC function.

Introduction

All cells of hematopoietic tissues are produced from a limited number of hematopoietic stem cells (HSC), which are localized mostly in the bone marrow (BM). HSC are mainly present as relatively quiescent cells which can be rapidly activated into the cell cycle by infectious and other inflammatory stress events. To prevent premature exhaustion due to replicative stress, the organism ensures the maintenance of HSC self-renewal under stress conditions through the BM microenvironment, or niche, which limits HSC proliferation and differentiation and promotes self-renewal.[1,2] The precise signals and mechanisms through which the niche exerts these HSC regulatory activities have not yet been worked out in detail.

Important mediators of HSC regulation by the niche are secreted members of the WNT family. The BM niche secretes both WNT-agonists and WNT-factor-binding antag-

onists such as the secreted frizzled-related proteins (SFRP).[3] SFRP1 is a secreted glycoprotein member of the SFRP family. In the BM microenvironment, SFRP1 is mainly expressed by mesenchymal stem and progenitor cells (MSPC) and osteoblastic cells.[4,5] Recent single-cell expression studies have shown that *Sfrp1* expression is mainly restricted to multipotent CXCL12-abundant reticulocytes (CAR cells).[6]

Secreted SFRP1 modulates the WNT signaling pathway through direct binding to either WNT or FZD receptors,[7] or within the cytoplasm, by interacting with Catenin beta-1 (β-catenin).[7,8] SFRP1 is mainly known as an inhibitor of canonical WNT signaling, which is characterized by the translocation of β-catenin into the cell nucleus. Here, β-catenin acts as a transcriptional coactivator in different transcription complexes, also called the WNT enhanceosome,[9] which governs transcription of WNT target genes.[10-13] The β-catenin enhanceosome also contains co-regulator proteins (CREB)-binding protein (CREBBP or CBP) or the closely related binding protein p300 (EP300).[14-16] Of these, CBP has been shown to be crucial for HSC self-renewal, while p300 is important for differentiation and senescence in HSC differentiation,[17,18] and the loss of p300 promotes the transition from myelodysplastic syndrome into acute myeloid leukemia.[19] The β-catenin/p300 interaction is increased by WNT ligands through elevating phosphorylation at Ser89 on p300.[20]

We have previously shown that deletion of the *Sfrp1* gene in mice reduces HSC self-renewal, leading to stem cell exhaustion.[21] Furthermore, in many different cancers, SFRP1 is down-regulated due to hypermethylation of the promoter region of the human *SFRP1* gene, leading to its decreased activity.[22-24] Since *Sfrp1* in the BM is mainly expressed by MSPC, we were interested in a more precise assessment of the deleterious effects of deletion of *Sfrp1* specifically in osteoprogenitors. Here, we found that Sfrp1 expression in osteogenic niche cells is required for optimal HSC self-renewal and differentiation upon engraftment, by extrinsic modulation of HSC proliferation through pSer89-p300 modulated by PP2A-PR72/130. Importantly, pharmacological treatment completely restored HSC repopulation in serial transplantations.

Methods

Animal studies

*Sfrp1*fl/fl mice were crossed with Osx-GFP::Cre mice (Osx-Cre; Jackson Labs, Bar Harbor, ME, USA).[25] Litters of Osx-Cre; *Sfrp1*fl/+ mice were crossed with *Sfrp1*fl/fl (S1fl/fl) mice so that litters yielded controls (S1fl/fl, and Osx-Cre [OS1+/+]) as well as *Sfrp1*-deleted mutants (OS1Δ/Δ). The results from S1fl/fl and OS1+/+ mice were combined as controls (CTRL). Further details are presented in the *Online Supplementary*

Methods.
Competitive repopulation was performed using transplantation of long-term (LT)-HSC into lethally irradiated (8.5 Gy) 129Ly5.1 wild-type (WT) recipient mice, as described previously.[26,27] Peripheral engraftment of donor cells was analyzed at regular intervals. Twenty-four weeks after transplantation, recipient mice were sacrificed and the hematopoietic organs were analyzed by flow cytometry. All animal experiments were approved by the Government of Upper Bavaria and performed in accordance with ethical guidelines and approved protocols (Vet_02-14-112, and -17-124). All animals were housed under specific pathogen-free conditions, according to the Federation of Laboratory Animal Science Associations and institutional recommendations. Mice used were 8 to 10 weeks old.

Flow cytometry and cell sorting

Hematopoietic Lineage⁻ SCA1+ KIT+ (LSK) cells and their HSC-enriched CD34⁻ CD48⁻ CD150+ subpopulations (LT-HSC) were isolated and labeled as reported elsewhere.[26,28] All antibodies used in this study are listed in *Online Supplementary Table S1*.
Peripheral blood (PB) was analyzed in an Animal Blood Cell Counter (Scil Vet Abc).

Single-cell cultures

Single LT-HSC were sorted and cultured in conditioned medium and cytokines as described previously,[27] before assays. More details can be found in the *Online Supplementary Methods*.

Hematopoietic colony assay

Cells from the single-cell culture assay or sorted LT-HSC (1x10³) were added to MethoCult™ GF M3434. After 10 to 14 days, colonies formed were counted under a microscope at 100-fold magnification according to standard criteria.

Assessment of DNA damage

Sorted LT-HSC were tested upon nucleic acid damage by single-cell gel electrophoresis (Comet Assay/Cell Biolab). Fluorescence images were taken using a Leica DM RBE microscope with AxioVision software (Carl Zeiss). DNA damage was analyzed by measuring the shift between the comet head (nucleus) and resulting tail (DNA damage).

Immunocytofluorescence staining

Hematopoietic cells were prepared and stained as described elsewhere.[26,28] The antibodies used are listed in *Online Supplementary Table S1*. Pictures were taken using a Leica DM RBE microscope with AxioVision software using standardized exposure settings for all samples. Thirty randomly captured cells per sample were imaged at 100-fold magnification. Confocal fluorescence micro-

scopy and deconvolution of the fluorescent images were performed on a Leica SP8 confocal microscope. Assessment of different parameters is outlined in the *Online Supplementary Methods*.

In vivo treatment with IQ-1

In *in vivo* experiments, the PR72/130-binding inhibitor IQ-1 (14 μg/mouse, Selleckchem, S8248) was administered intraperitoneally every 24 h for 5 consecutive days.

RNA sequencing and data analysis

RNA sequencing was performed with 800 to 1,000 sorted LT-HSC. Details are provided in the *Online Supplementary Methods*. All analyses were performed in python and the R statistical environment (*http://www.R-project.org*).

Statistical analyses

Statistical tests are indicated in the figure legends. The software used for the computations was GraphPad (La Jolla, CA, USA). *P* values less than or equal to 0.05 were considered to be statistically significant. Data are presented as the mean ± standard deviation.

Results

Targeted deletion of the *Sfrp1* gene in mesenchymal stem and progenitor cells *in vivo*

The *Sfrp1* gene is highly expressed in CD45⁻Ter119⁻CD31⁻CD166⁻SCA-1⁺ MSPC compared to CD45⁻Ter119⁻CD31⁻CD166⁺SCA-1⁺ osteoblastic cells (OBC) and CD45⁻Ter119⁻CD31⁺SCA-1⁺ endothelial cells (EC) from WT mice (*Online Supplementary Figure S1A-C*). For generation of mice with conditional alleles of the *Sfrp1* gene, we used the mutant C57Bl/6N-ES cell clone in which exon 2 of the *Sfrp1* gene was flanked with loxP sites. The resulting *Sfrp1*^fl/fl mice were crossed with mice expressing *CRE eGFP* under the continuous control of the promotor for the osteoprogenitor gene Osterix (gene name *Sp7*) (OS1^Δ/Δ; *Online Supplementary Figure S1D, E*). We verified deletion of *Sfrp1* in sorted and cultured MSPC from OS1^Δ/Δ and control mice via immunostaining and western blot (*Online Supplementary Figure S1F-I*). Mouse embryonic fibroblasts from *Sfrp1* knockout mice and their WT littermates were used for antibody verification (*Online Supplementary Figure S1J*). OS1^Δ/Δ mice are viable and fertile and show unaltered prenatal development (*Online Supplementary Figure S2A*). However, 8-week-old OS1^Δ/Δ mice were smaller and weighed less than their Cre⁻ littermates, regardless of sex (*Online Supplementary Figure S1A, B*). Since a previous study[29] had shown that *Sfrp1* expression is critical for skeletogenesis in mice, we analyzed bone homeostasis in OS1^Δ/Δ mice and controls at 8 weeks of age (*Online Supplementary Figure S2C-F*). We found that 8-week-old

OS1^Δ/Δ mice show mild, but significantly reduced femur length, and reduced serum levels of CTX (a bone resorption marker) (*Online Supplementary Figure S2C, E*). However, trabecular parameters and serum P1NP (a bone formation marker) (*Online Supplementary Figure S2D, E*) were not affected. Similarly, the numbers of TRAP-positive osteoclasts and osteoblasts on the bone surface were not different between OS1^Δ/Δ and control mice (*Online Supplementary Figure S2F*), indicating that there are no major defects in bone formation in 8-week-old OS1^Δ/Δ animals. To assess the effect of *Sfrp1* deletion on MSPC function, we first scored the frequency of BM colony-forming unit fibroblasts (CFU-F) (*Online Supplementary Figure S3A*). Interestingly, where the total number of sorted OS1^Δ/Δ MSPC was decreased in the BM (*Online Supplementary Figure S3B*), the number of small CFU-F-derived colonies (up to 50 cells) was significantly increased (*Online Supplementary Figure S3C*). When we stained the colonies after scoring for senescence, we detected an increased number of senescent colonies in OS1^Δ/Δ mice compared to control mice (*Online Supplementary Figure S3D*), suggesting that more OS1^Δ/Δ CFU-F are in a pre-senescent state.

Hematopoiesis in mice with loss of *Sfrp1* in bone marrow niche cells

We next investigated how the loss of *Sfrp1* in MSPC and osteoprogenitors affects the hematopoietic compartment under steady-state conditions. An initial analysis of the PB and BM of the OS1^Δ/Δ mice and control animals showed that the white blood cell counts and total cell numbers of the BM were unchanged (*Online Supplementary Figure S4A*). In addition, the percentages of B220⁺ B cells and myeloid cell populations (GR1^medCD11b⁺ monocytes and GR1⁺CD11b⁺ granulocytes) of the OS1^Δ/Δ mice and controls were similar in both PB and BM. Circulating T cells were slightly increased in the PB but not in the BM of OS1^Δ/Δ mice (*Online Supplementary Figure S4B-D*). Furthermore, the numbers of the earliest hematopoietic cells, LSK, CD34⁻CD48⁻CD150⁺ LSK (LT-HSC) and CD34⁺CD48⁻ LSK (ST-HSC), were unchanged in OS1^Δ/Δ mice compared to control mice. However, under these steady-state conditions, we observed a significant decrease in the number of SCA1⁻ myeloid progenitor cells (Lin⁻SCA1⁻KIT⁺) (*Online Supplementary Figure S4E, F*) in OS1^Δ/Δ mice, suggesting reduced transition of stem cells into the myeloid progenitor cell compartment.

Long-term hematopoietic stem cells from OS1^Δ/Δ mice show strongly reduced repopulation activity

To test whether deletion of *Sfrp1* in MSPC and osteoprogenitors indirectly affects stem cell repopulation activity, we transplanted 100 sorted LT-HSC from OS1^Δ/Δ or control mice into lethally irradiated WT recipients (Figure 1A). These experiments showed that peripheral engraftment

from OS1$^{\Delta/\Delta}$ LT-HSC was severely impaired throughout the 24-week observation period (Figure 1B, C). Furthermore, donor engraftment of OS1$^{\Delta/\Delta}$ cells was dramatically reduced in the BM of recipient mice 24 weeks after transplantation, as compared with the engraftment in control mice (Figure 1B, D). The failed repopulation of transplanted OS1$^{\Delta/\Delta}$ LT-HSC was possibly driven by significantly lower regeneration of ST-HSC and LT-HSC compared to that of transplanted control LT-HSC. It is notable that seven out of ten recipient mice transplanted with OS1$^{\Delta/\Delta}$ LT-HSC showed a complete absence of a donor LT-HSC compartment (Figure 1E, F).

Since LT-HSC with reduced repopulating activity are frequently found to have DNA damage,[30,31] we analyzed DNA damage in sorted LT-HSC from OS1$^{\Delta/\Delta}$ and control mice (Figure 2A). Interestingly, LT-HSC from OS1$^{\Delta/\Delta}$ mice displayed an increased number of phosphorylated foci on histone H2A.X (γH2A.X) and longer DNA fragment tails in the comet assay, indicating DNA double-strand breaks in LT-HSC from OS1$^{\Delta/\Delta}$ mice (Figure 2B, C). These results suggest that LT-HSC from OS1$^{\Delta/\Delta}$ mice may already be dysfunctional prior to transplantation.
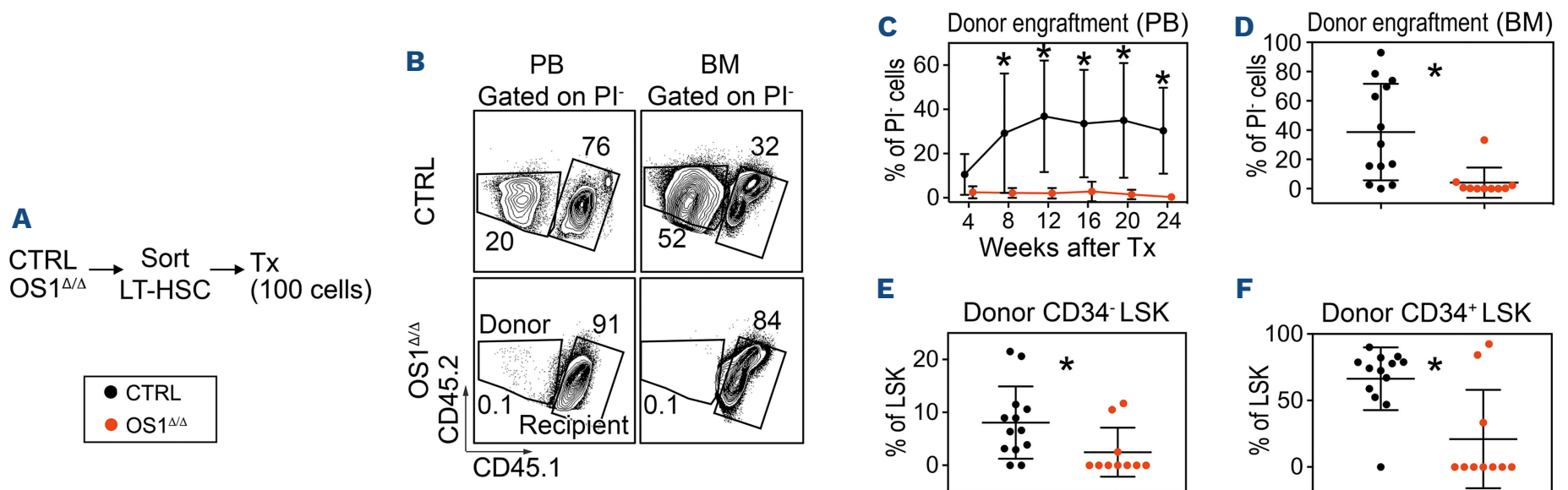
Figure 1. Long-term hematopoietic stem cells from OS1$^{\Delta/\Delta}$ mice failed to repopulate in wild-type recipients. (A) Experimental design: long-term hematopoietic stem cells (LT-HSC) from 8- to 10-week-old OS1$^{\Delta/\Delta}$ mice and control animals (CTRL, *Sfrp1*$^{fl/fl}$) were sorted and transplanted into lethally irradiated wild-type recipients. (B) Representative flow cytometry plots of the gating strategy of Ly5.2$^+$ donor cells or Ly5.1$^+$Ly5.2$^+$ recipient cells in peripheral blood (left) and bone marrow (right). (C) Percentage donor cell engraftment in the peripheral blood 4, 8, 12, 16, 20 and 24 weeks after transplantation. (D) Percentage donor engraftment in bone marrow (week 24 after transplantation). (E) Percentage of donor CD34$^-$ LSK cells. (F) Percentage of donor CD34$^+$ LSK cells from OS1$^{\Delta/\Delta}$ mice (n=10) compared to control mice (n=13). Each dot represents one animal (D-F). Values are presented as the mean ± standard deviation. *$P\leq0.05$ indicates a statistically significant difference determined by an unpaired *t* test. Symbol legends are as shown in (A). CTRL: littermate WT controls; LT-HSC: long-term hematopoietic stem cells; Tx: transplantation; PB: peripheral blood; BM: bone marrow; PI: propidium iodide.
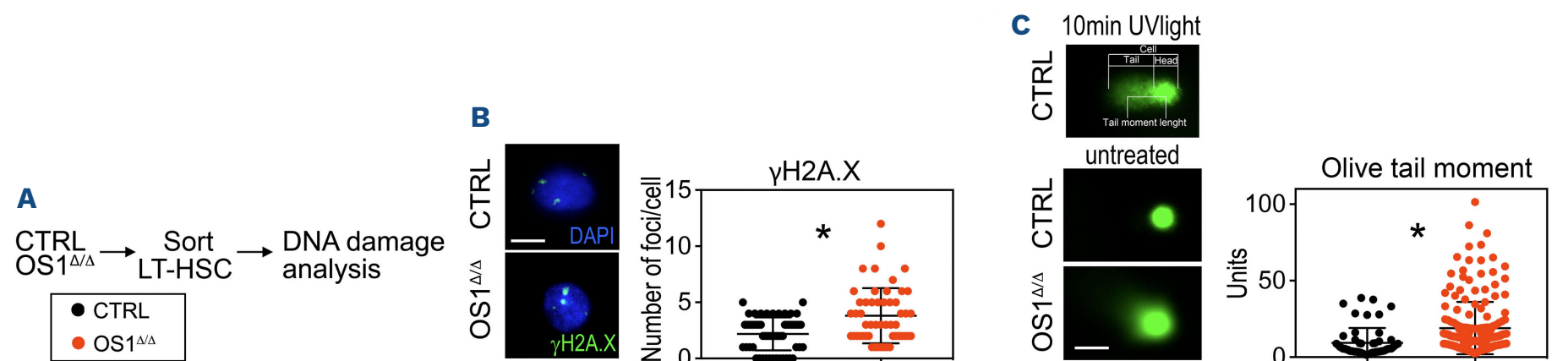
Figure 2. Long-term hematopoietic stem cells from OS1$^{\Delta/\Delta}$ mice showed DNA damage. (A) Experimental design: long-term hematopoietic stem cells (LT-HSC) from 8- to 10-week old OS1$^{\Delta/\Delta}$ mice and controls (*Sfrp1*$^{fl/fl}$) were sorted and analyzed for DNA damage. (B) Left. Representative immunofluorescence staining for nuclei staining with DAPI in blue and histone γH2A.X foci content in green of LT-HSC. Right. Number of histone γH2A.X foci content of LT-HSC of OS1$^{\Delta/\Delta}$ mice (n=52) compared to controls (n=59). (C) Left. Immunofluorescence staining of a positive control (cells treated with UV light for 10 min), top. Representative immunofluorescence staining of cells from OS1$^{\Delta/\Delta}$ mice compared to those from control mice; below. Right. Units of olive tail moment (tail DNA/cell DNA * TML) of LT-HSC from OS1$^{\Delta/\Delta}$ mice (n=200) compared to control mice (n=55) calculated after a comet assay. Each dot represents one cell (B, C). Values are presented as means ± standard deviation. *$P\leq0.05$ indicates a statistically significant difference determined by an unpaired *t* test. Scale bar: 5 µm. Symbol legends as shown in (A). CTRL: control mice.

Loss of function of hematopoietic stem cells from OS1$^{\Delta/\Delta}$ mice *in vitro*

To investigate the survival, proliferation and differentiation of LT-HSC from OS1$^{\Delta/\Delta}$ mice, we set up single-cell cultures (Figure 3A, D).[27,32] In the first experiments, we investigated whether knocking down *Sfrp1* in stromal cells alters the potential of conditioned medium to maintain LT-HSC. To do this, we used medium conditioned on the HSC supportive stromal cell line UG26-1B6[33,34] with knockdown-*Sfrp1* (sh*Sfrp1*) or control cells (*pLKO.1*) (Figure 3A). Interestingly, WT LT-HSC cultured in sh*Sfrp1* UG26-1B6 conditioned medium, stem cell factor (KITL), and interleukin-11 showed unchanged survival, but decreased clone size compared to WT LT-HSC cultured in control conditioned medium (Figure 3B, C). Next, we analyzed LT-HSC from OS1$^{\Delta/\Delta}$ mice compared to control LT-HSC in UG26-1B6 conditioned medium (Figure 3A). In this case, we found that LT-HSC from OS1$^{\Delta/\Delta}$ mice show decreased clone size after 4 and 5 days of culture compared to LT-HSC from control mice (Figure 3D). Importantly, we found a significant decrease in colonies grown from pooled day 6 clones of OS1$^{\Delta/\Delta}$ LT-HSC (Figure 3E) as well as a significantly decreased proportion of LSK cells and myeloid progenitors in these colonies compared to the control LT-HSC (Figure 3F, G). These results support the view that LT-HSC from OS1$^{\Delta/\Delta}$ mice have reduced proliferation with decreased colony formation.

To gain insights into the possible molecular mechanisms of reduced proliferation in LT-HSC from OS1$^{\Delta/\Delta}$ mice, we further investigated the expression of β-catenin co-activating acetylases CREBBP (CBP) and EP300 (p300) in LT-
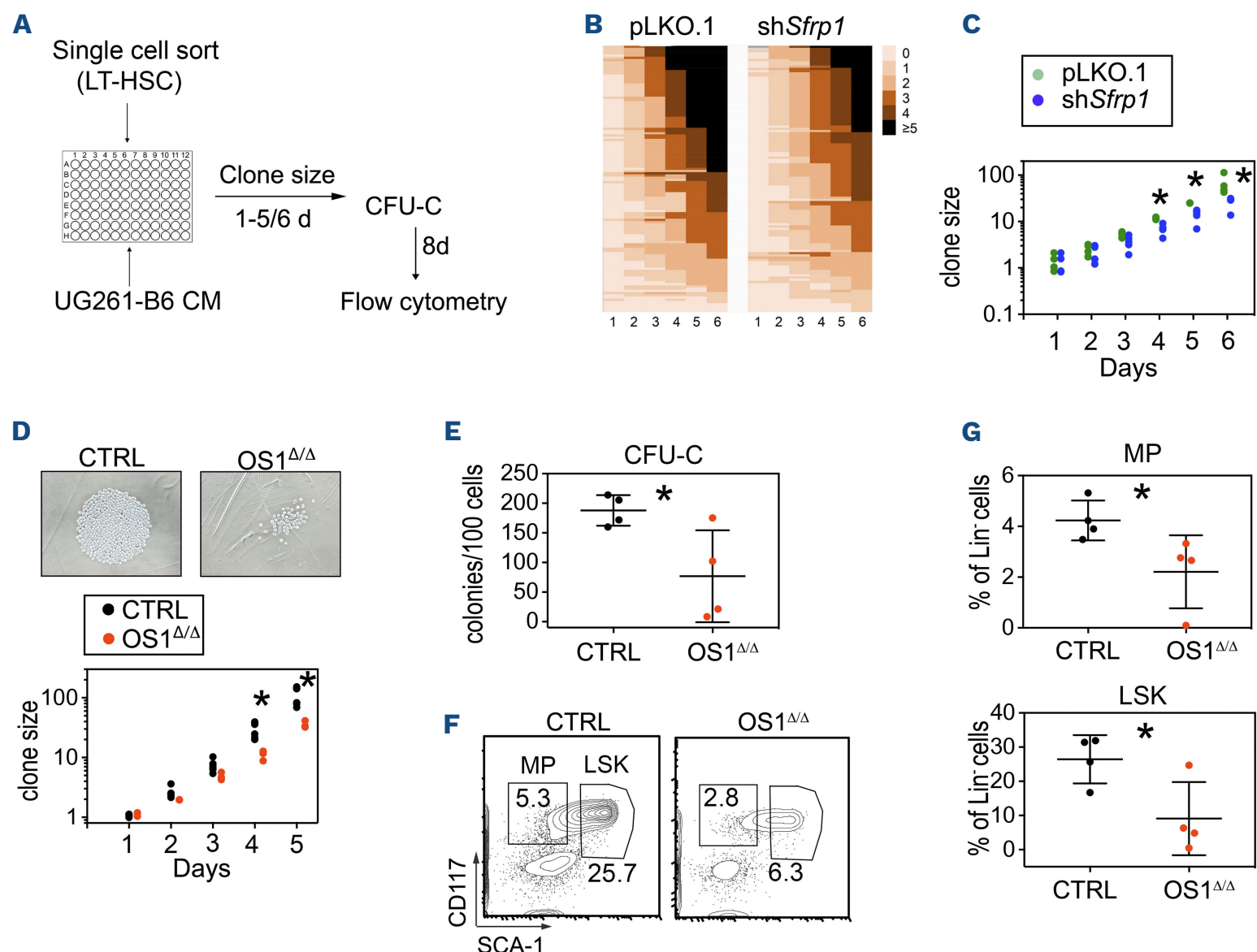
Figure 3. Long-term hematopoietic stem cells from OS1$^{\Delta/\Delta}$ mice proliferate slowly. (A) Experimental design: details can be found in the Methods. (B) Representative heat maps of the minimal number of cell divisions per clone per well for each long-term hematopoietic stem cell at each day of culture in pLKO.1 (left), or in sh*Sfrp1* UG26-1B6 conditioned medium (right). (C) Counted mean clone size per well over 6 days of wild-type cells in pLKO.1 or in sh*Sfrp1* UG26-1B6 conditioned medium (n=6). (D) Top. Representative picture of cells on day 5 of culture. Bottom: counted mean clone size over 5 days from OS1$^{\Delta/\Delta}$ mice (n=3) and controls (n=6). (E) Counted total numbers of colonies from OS1$^{\Delta/\Delta}$ mice (n=4) and controls (*Sfrp1$^{fl/fl}$*) (n=4) in M3434 after 8 days of culture after 5 days of single-cell culture. (F) Representative flow cytometry plots of harvested cells after 8 days of methylcellulose culture of cells from control mice (left) and OS1$^{\Delta/\Delta}$ mice (right). (G) Percentages of myeloid progenitors (top) and LSK cells (bottom) in harvested cells after 8 days culture in M3434 of cells from OS1$^{\Delta/\Delta}$ mice (n=4) and control mice (n=4). Each dot represents one animal (E, G) or plate (C, D). Values represented in the graphs are means ± standard deviation. *P≤0.05 indicates a statistically significant difference determined by an unpaired *t* test. Symbol legends as shown in (C). LT-HSC: long-term hematopoietic stem cells; CM: conditioned medium; CFU-C: colony-forming unit-cells; CTRL: control; MP: myeloid progenitors.

HSC (Figure 4A), proteins which are known to regulate proliferation and differentiation in embryonic stem cells,[35] self-renewal of HSC,[17] and senescence in fibroblasts.[18] These experiments showed that in sorted LT-HSC from OS1[Δ/Δ] mice, the protein levels of both β-catenin and p300 were elevated, while the level of CBP remained unchanged (Figure 4B-D). This suggests that due to the increased expression of p300, CBP-driven self-renewal may be reduced in LT-HSC from OS1[Δ/Δ] mice compared to control mice.

### Restoration of hematopoietic stem cell quality with IQ-1 treatment *in vivo*

Phosphorylation of p300 at position Ser89 is known to stabilize the interaction between β-catenin and p300.[20,35] Considering that p300 reduces cell proliferation and promotes differentiation and senescence, IQ-1 has been used to reduce the phosphorylation of Ser89-p300 and, by doing so, indirectly to decrease the activity of the β-catenin/p300 enhanceosome. Interestingly, IQ-1 does not reduce transcriptional activity by binding to p300 directly, but instead it binds to PR72/130 (PPP2R3A), a regulatory subunit of the serine/threonine phosphatase PP2A, which is responsible for reducing pSer-p300.[35-38]

To reduce the amount of phospho-p300 *in vivo*, we treated mice for 5 days with IQ-1 via daily intraperitoneal injection[38] and analyzed differentiation and repopulating activity of LT-HSC (Figure 5A, B). We found that IQ-1 treatment did not affect control mice. In OS1[Δ/Δ] mice, IQ-1 did not affect the absolute numbers of ST-HSC and LT-HSC, while the number of myeloid progenitors was still decreased compared with that in control mice (Figure 5B-E, *Online Supplementary Figure S4F*). This suggests that IQ-1 does not affect steady-state hematopoiesis in either control or OS1[Δ/Δ] mice.

However, whereas IQ-1 did not affect pSer89-p300 in control LT-HSC, it significantly decreased pSer89-p300 after 5 days of treatment of LT-HSC from OS1[Δ/Δ] mice (Figure 5F); the protein levels of PPP2R3A and β-catenin were unaltered (*Online Supplementary Figure S1G-I*). To determine the clonogenic capacity of LT-HSC from untreated and IQ-1-treated primary recipient mice, sorted LT-HSC were plated in growth factor-supplemented methylcellulose. Here, we found that IQ-1treatment of donor mice improved colony formation of regenerated LT-HSC, in both control and OS1[Δ/Δ] mice (Figure 5G), indicating that clonogenic hematopoietic activity in regenerated donor OS1[Δ/Δ] LT-HSC is restored to control levels by *in vivo* IQ-1 treatment.

To identify possible underlying molecular changes of the effects of IQ-1 treatment, we analyzed the transcriptome of 500-1000 LT-HSC before and after treatment with IQ-1
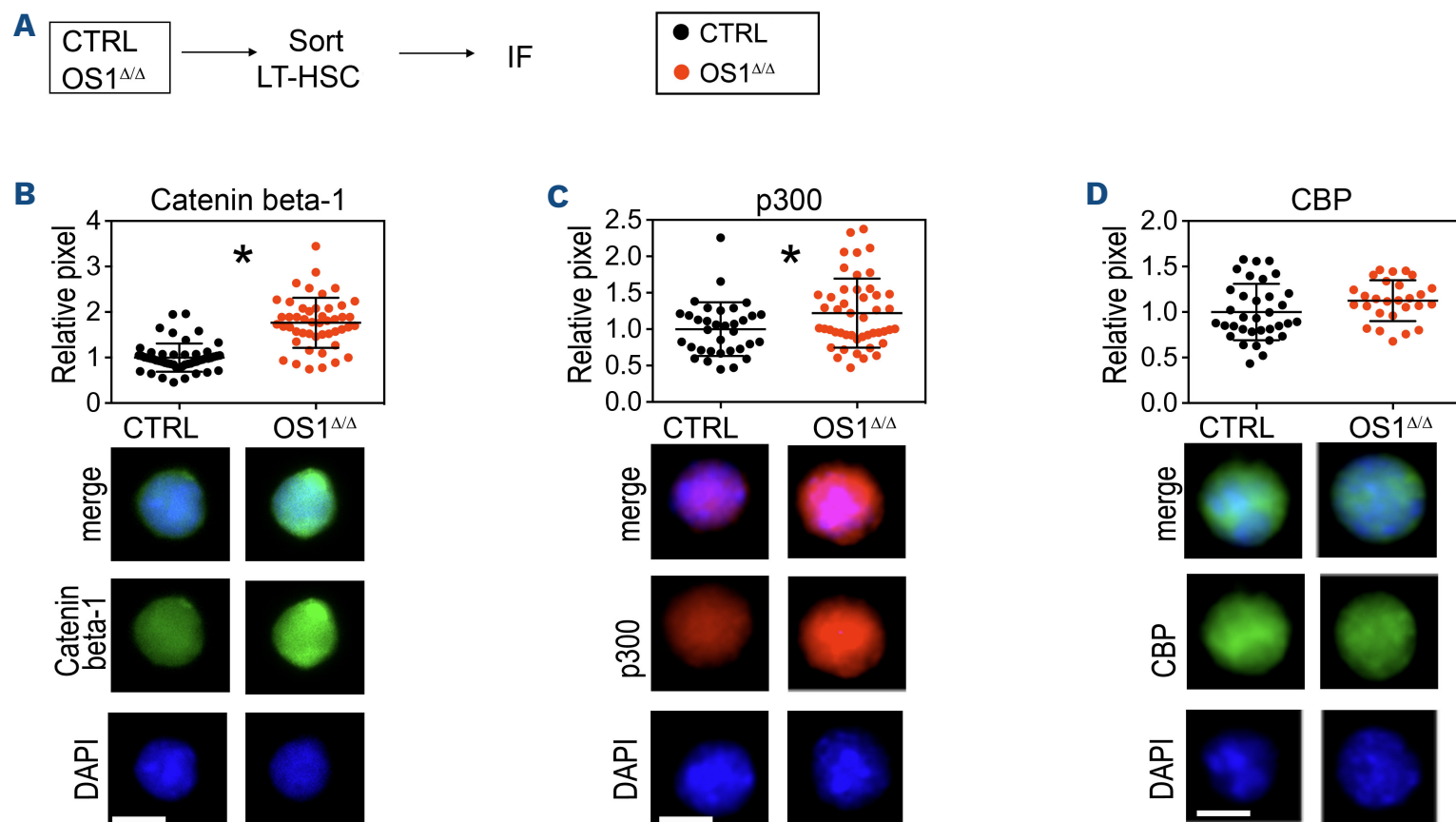
Figure 4. Enhanced β-catenin/p300 signaling in long-term hematopoietic stem cells from OS1[Δ/Δ] mice. (A) Experimental design of immunofluorescence staining of long-term hematopoietic stem cells (LT-HSC) from OS1[Δ/Δ] and control (*Sfrp1^{fl/fl}*) mice for (B) catenin beta-1 (β-catenin), (C) p300 and (D) CBP protein content as pixel number of 50-60 LT-HSC sorted from the bone marrow of OS1[Δ/Δ] mice and control mice with representative immunofluorescence nuclei staining with DAPI in blue (bottom), protein of interest in green (middle), and the merged picture (top). Each dot represents one cell (B-D). Values in the graphs are means ± standard deviation. *P≤0.05 indicates a statistically significant difference determined by an unpaired *t* test. Scale bar: 5 μm. Symbol legends as shown in (A). CTRL: control; IF: immunofluorescence; CBP: CREB-binding protein.
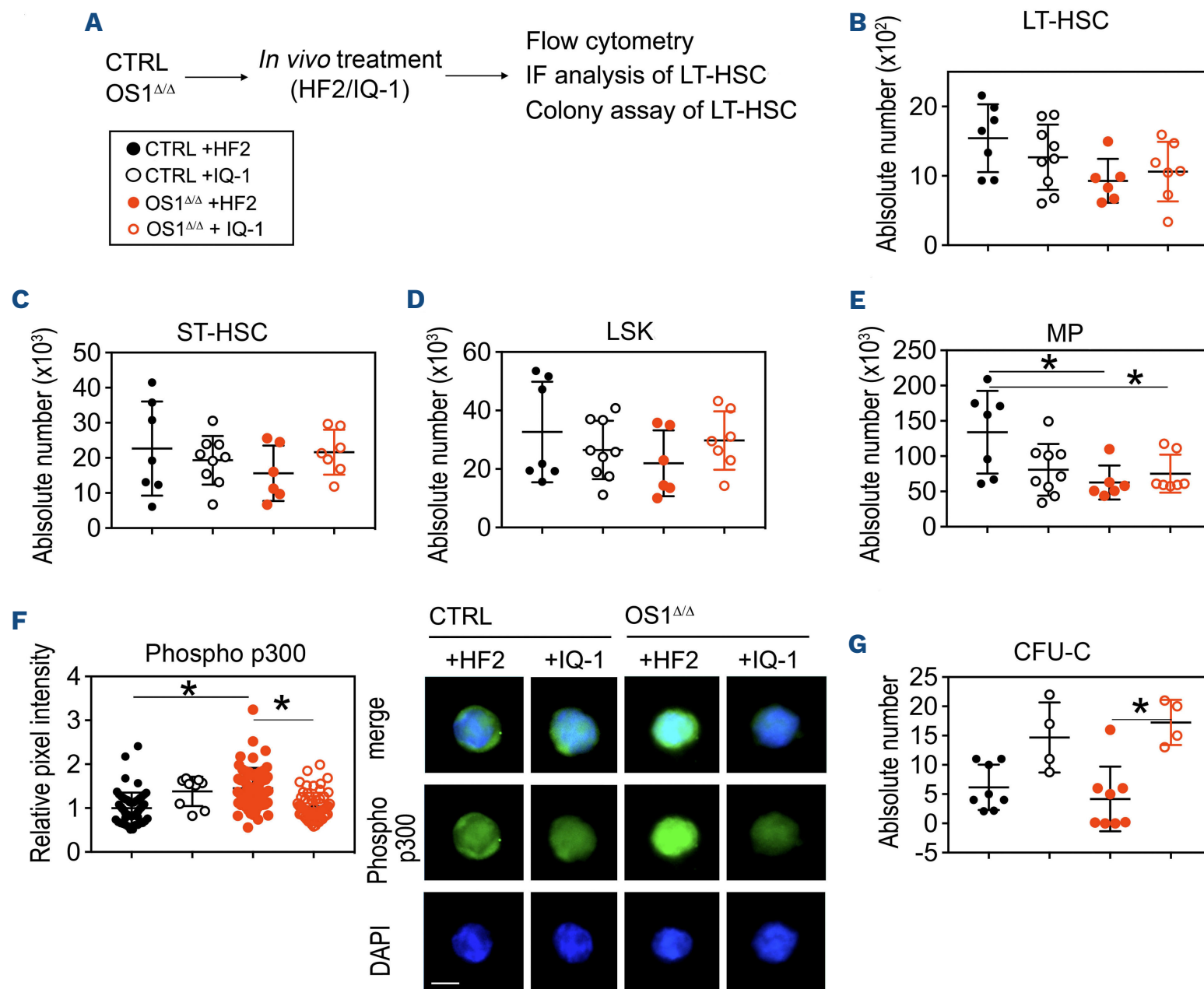
Figure 5. The impact of IQ-1 treatment on the primitive hematopoietic compartment of the bone marrow. (A) Experimental design of the *in vivo* IQ-1 treatment: 8- to 10-week-old OS1$^{\Delta/\Delta}$ mice and control mice (*Sfrp1*$^{fl/fl}$) were injected intraperitoneally with IQ-1 (14 µg) or vehicle (HF2) for 5 days. The composition of the primitive hematopoietic compartment of the bone marrow was analyzed 24 hours later. (B) Absolute number of long-term hematopoietic stem cells (LT-HSC); (C) absolute number of short-term hematopoietic stem cells; (D) absolute number of LSK cells; and (E) absolute number of myeloid progenitors of OS1$^{\Delta/\Delta}$ mice; (HF2: n=6; IQ-1: n=7) compared to those from controls (HF2: n=7; IQ-1: n=9). (F) Left. Phospho-p300 protein content as relative pixel number of LT-HSC from IQ-1-treated and untreated OS1$^{\Delta/\Delta}$ mice (HF2: n=60; IQ-1: n=60) and control mice (HF2: n=60; IQ-1: n=60). Right. Representative immunofluorescence staining for the nuclei staining with DAPI in blue (bottom), phospho-p300 protein in green (middle), and the merged picture (top) of LT-HSC from IQ-1-treated and untreated OS1$^{\Delta/\Delta}$ mice and controls. (G) Counted total numbers of colony-forming unit-cells from IQ-1-treated and untreated OS1Δ/Δ mice (HF2: n=8; IQ-1: n=4) and control animals (HF2: n=8; IQ-1: n=4). Each dot represents one animal (B-E, G) or cell (F). The values shown are means ± standard deviation. *$P \leq 0.05$ indicates a statistically significant difference determined by analysis of variance, with a Tukey *post-hoc* test. Scale bar: 5 µm. Key to symbols as shown in (A). CTRL: control; IF: immunofluorescence; ST-HSC: short-term hematopoietic stem cells; MP: myeloid progenitors; CFU-C: colony-forming unit-cell.

via RNA sequencing (*Online Supplementary Figure S5A*). Global gene set enrichment analysis showed that the gene sets 'E2F_target', and 'G2M checkpoints' were significantly enriched in control LT-HSC, whereas 'Reactive oxygen species pathway' was enriched in OS1$^{\Delta/\Delta}$ LT-HSC (*Online Supplementary Figure S5B-D*). However, the expression of the differentially regulated genes from these gene sets (*Online Supplementary Figure S5E-G*) was not completely restored in IQ-1-treated animals.

Since IQ-1 affects post-translational modifications through PP2A and such modifications modify protein-pro-

tein interactions, we then looked more closely at subcellular protein levels and localization. For this purpose, LT-HSC were sorted from control and OS1$^{\Delta/\Delta}$ mice treated with IQ-1 or the vehicle (HF2) (Figure 6A). Confocal analysis of PPP2R3A (PR72/130) and p300 not only showed p300 upregulation in OS1$^{\Delta/\Delta}$ LT-HSC (see also Figure 4C), but also its co-localization with PR72/130 and a strongly increased nuclear presence of p300 in OS1$^{\Delta/\Delta}$ LT-HSC (Figure 6B-D and *Online Supplementary Videos*). In LT-HSC from IQ-1-treated control or OS1$^{\Delta/\Delta}$ mice, both nuclear p300 and PR72 co-localization with p300 was similar to that of un-

treated controls, indicating restoration of both nuclear accumulation of p300 and co-localization with PR72/130 by IQ-1 treatment. We then assessed whether pSer89-p300 would also associate more with β-catenin, and found a stronger association in OS1$^{\Delta/\Delta}$ LT-HSC (Figure 6E, F), indicating increased activity of the β-catenin/p300 complex. In LT-HSC from IQ-1-treated OS1$^{\Delta/\Delta}$ mice, this association was significantly lower, showing that IQ-1 reduces the interaction of p300 and β-catenin.

We then investigated whether the identified changes are sufficient to restore the repopulation activity of LT-HSC from IQ-1-treated OS1$^{\Delta/\Delta}$ mice (Figure 7A). In line with this hypothesis, we observed that donor LT-HSC from these mice repopulated to a similar extent as LT-HSC from untreated control mice, whereas LT-HSC from untreated OS1$^{\Delta/\Delta}$ mice did not engraft (Figure 7B, C). Importantly, LT-HSC from IQ-1-treated OS1$^{\Delta/\Delta}$ mice were now able to efficiently regenerate the donor stem and progenitor compartments in recipient BM (Figure 7D). Interestingly, the absolute number of donor-derived CD34$^-$ LSK cells and donor-derived myeloid progenitors of transplanted LT-HSC from IQ-1-treated OS1$^{\Delta/\Delta}$ mice was even higher than that of the donor-derived CD34$^-$ LSK cells and myeloid progenitors from transplanted control LT-HSC (Figure 7E-H).

We next investigated the clonogenic ability of the regenerated donor cells (*Online Supplementary Figure S6A*). In line with the observations described above, regenerated OS1$^{\Delta/\Delta}$ donor LSK cells formed very few colonies, whereas the colony-forming ability of LSK cells from regenerated cells from the IQ-1-treated OS1$^{\Delta/\Delta}$ mice was similar to that of the control donor LSK cells (*Online Supplementary Figure S7B*). On a molecular level, both phospho-p300 (Ser89) content and the number of γH2A.X foci were similar in regenerated LT-HSC from IQ-1-treated OS1$^{\Delta/\Delta}$ or control donor mice (*Online Supplementary Figure S6C, D*).

To determine whether IQ-1 treatment of dysfunctional HSC in OS1$^{\Delta/\Delta}$ mice not only restores their engraftment in primary recipients, but also their long-term self-renewal activity, we transplanted donor HSC from primary recipients, and transplanted these into secondary WT recipient mice (Figure 8A, *Online Supplementary Figure S7A*). For this purpose, 1,000 (Figure 8) or 2,000 (*Online Supplementary Figure S7*) donor LSK cells were sorted from the BM of recipient mice transplanted with LT-HSC from either IQ-1-treated OS1$^{\Delta/\Delta}$ (n=8) or untreated control mice (n=9). We found that IQ-1 treatment of OS1$^{\Delta/\Delta}$ donors not only restored multilineage engraftment of the primary recipients (Figure 7), but also the long-term repopulating ability
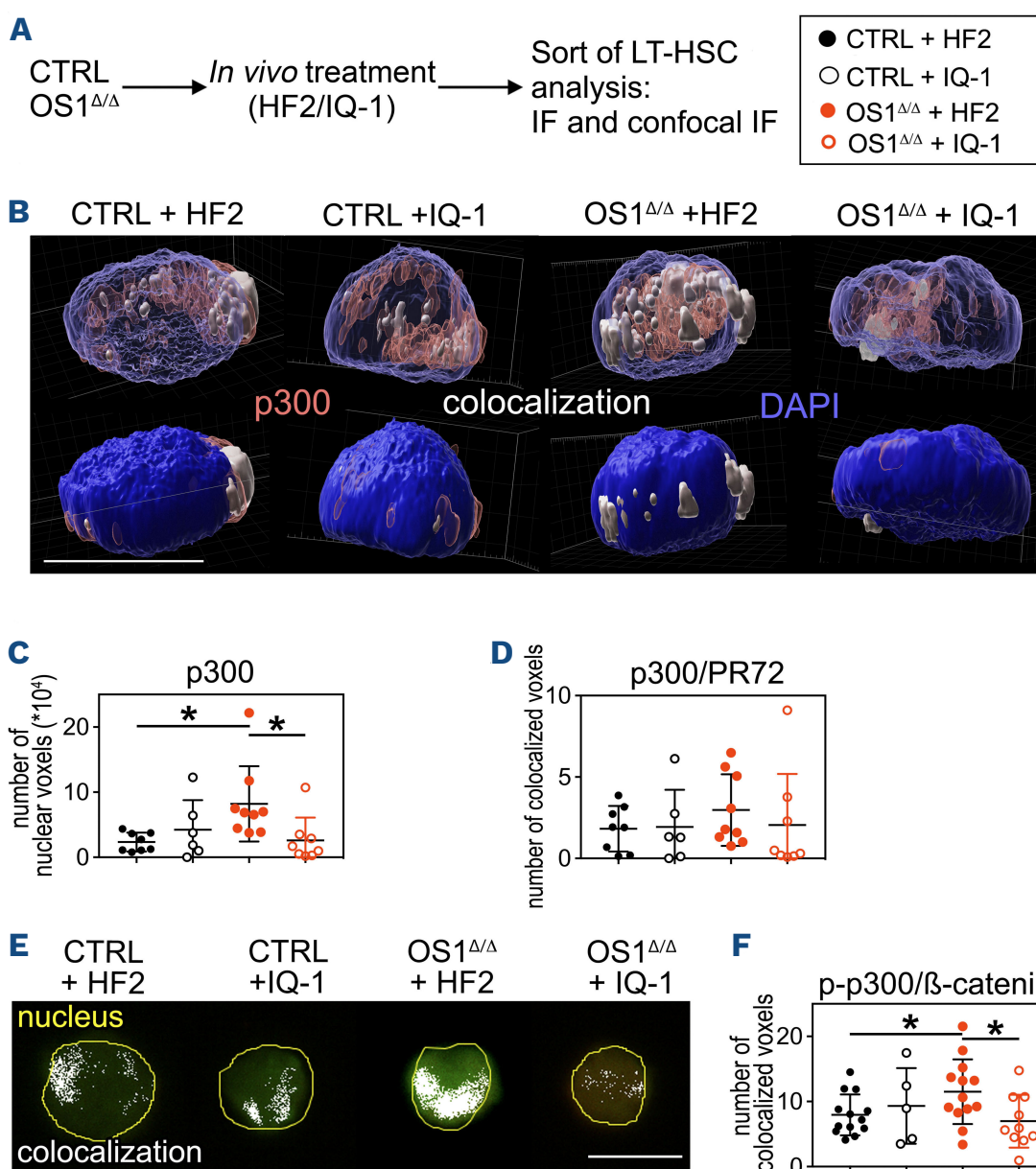

Figure 6. The impact of IQ-1 treatment on the p300 signaling pathway. (A) Experimental design of the *in vivo* IQ-1 treatment: 8- to 10-week-old OS1$^{\Delta/\Delta}$ mice and control mice (*Sfrp1*$^{fl/fl}$) were injected intraperitoneally with IQ-1 (14 µg) or vehicle (HF2) for 5 days. The composition of the primitive hematopoietic compartment of the bone marrow was analyzed 24 hours later. (B) Confocal microscopy pictures of p300 protein (red) and colocalization with PR72 (white) of long-term hematopoietic stem cells (LT-HSC) from IQ-1-treated and untreated OS1$^{\Delta/\Delta}$ mice (HF2: n=30; IQ-1: n=30) and control mice (HF2: n=30; IQ-1: n=30, B-F). (C) Number of voxels of p300 in the nuclear area of LT-HSC from IQ-1-treated and untreated OS1$^{\Delta/\Delta}$ mice. (D) Number of colocalized voxels of p300 and PR72 in the cytoplasm of LT-HSC from IQ-1-treated and untreated OS1$^{\Delta/\Delta}$ mice. (E) Representative pictures of the immunofluorescence staining showing the colocalization of β-catenin and phospho-p300 (white) of LT-HSC from IQ-1-treated and untreated OS1$^{\Delta/\Delta}$ mice and controls. (F) Number of colocalized voxels of phospho-p300 and β-catenin of LT-HSC from IQ-1-treated and untreated control and OS1$^{\Delta/\Delta}$ mice. Scale bar: 5 µm. Each dot represents one cell. Values are presented as means ± standard deviation. *P≤0.05 indicates a statistically significant difference determined by the Mann-Whitney test. Symbol legends are as shown in (A). CTRL: control; IF: immunofluorescence.

in secondary recipients to levels comparable to those of the untreated WT controls (Figure 8B-I, *Online Supplementary Figure S7B-L*). Thus, the long-term repopulating ability of dysfunctional HSC from OS1[Δ/Δ] mice was completely restored by prior *in vivo* IQ-1 treatment of the OS1[Δ/Δ] donor mice.

Discussion

Our results show that deletion of *Sfrp1* expression in osteoprogenitors strongly reduces the colony-forming and repopulating ability of HSC. Our experiments link these findings to reduced proliferation in single-cell assays, and increased DNA damage. On a molecular level, both β-catenin and p300 levels were elevated, while CBP content was not affected. Mechanistically, we found an increased level of nuclear p300 and an enhanced presence of β-catenin/phospho-p300-containing colocalization, indicating increased p300 transcriptional activity. Furthermore, we provide evidence that interfering with this interaction by decreasing p300 phosphorylation at Serine 89 reverses the dysfunctional hematopoietic phenotype and restores long-term repopulating activity of HSC from OS1[Δ/Δ] mice. Our study shows that the PR72/130-binding inhibitor IQ-1 reduces nuclear p300 activity of HSC from OS1[Δ/Δ] mice. PR72 and PR130 are two proteins derived from the

Ppp2r3a gene, and both act as B regulatory subunits of PP2A phosphatase. PR72/130 promotes PP2A phosphatase activity.[39] PR72/130 binds to different substrates, including several involved in the DNA damage response and Wnt signaling.[39,40] It is of note that in our *in vivo* study, we found that IQ-1 treatment reduces the level of phospho-p300 in LT-HSC, suggesting that pSer89-p300 is a direct target of the PP2A-PR72/130 phosphatase in OS1[Δ/Δ] cells. To determine whether p300 activity is the main or even only target of IQ-1 treatment in HSC, more knowledge should be generated in the future about possible targets of this phosphatase in HSC. Nevertheless, our results show that the PP2A-PR72/130 phosphatase regulates the WNT-catenin enhanceosome through p300 phosphorylation in HSC.

In other cell systems, increased pSer89-p300 increases differentiation not only in embryonic stem cells,[35] but also in teratocarcinoma cells[41] and alveolar progenitors.[20] Furthermore, p300, but not CBP, has been found to induce a hyperacetylated chromatin state that promotes senescence.[18] Consistent with this, we found increased DNA damage, which is often found in senescent LT-HSC.[30,31] Self-renewal, on the other hand, requires a full dose of CBP,[17] and deletion of CBP results in HSC exhaustion.[17,42] In addition, specific inhibition of CBP eliminates cancer stem cells.[43] Although the observed effects of IQ-1 in reversing *in vivo* HSC dysfunction and reduction of nuclear p300 localization as well as pSer89-p300 and its association with
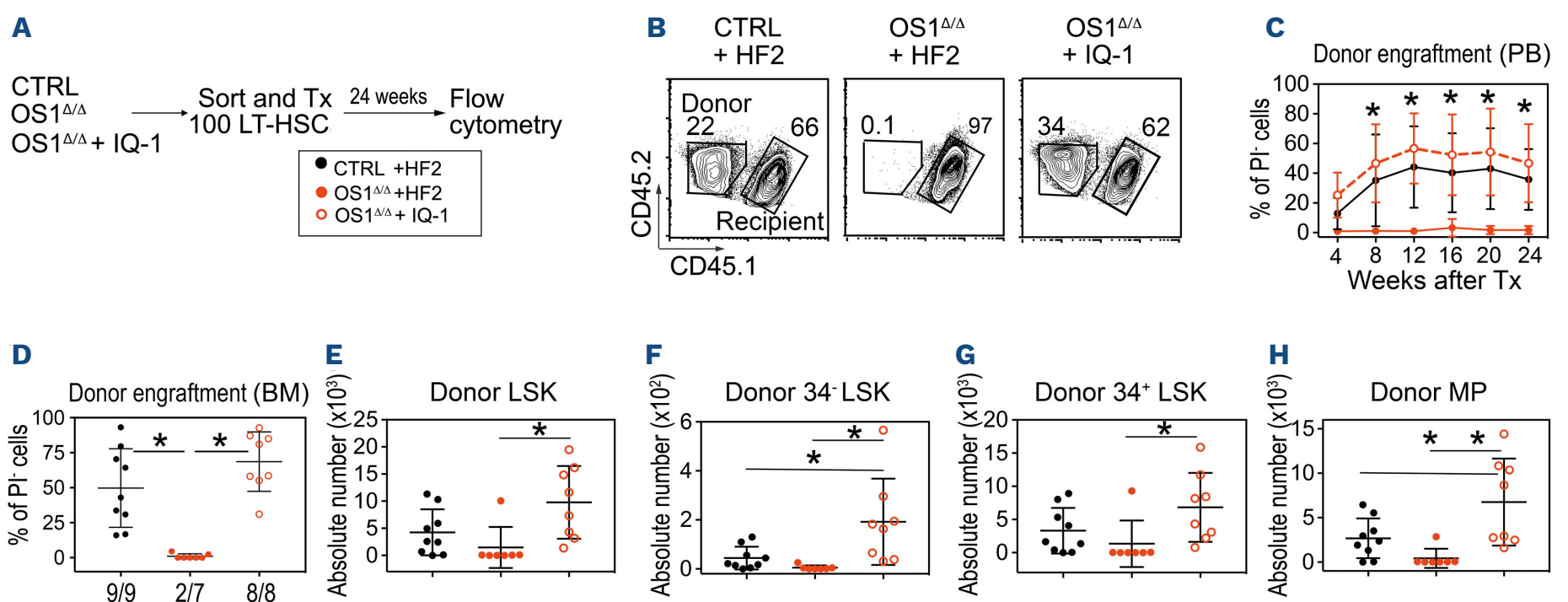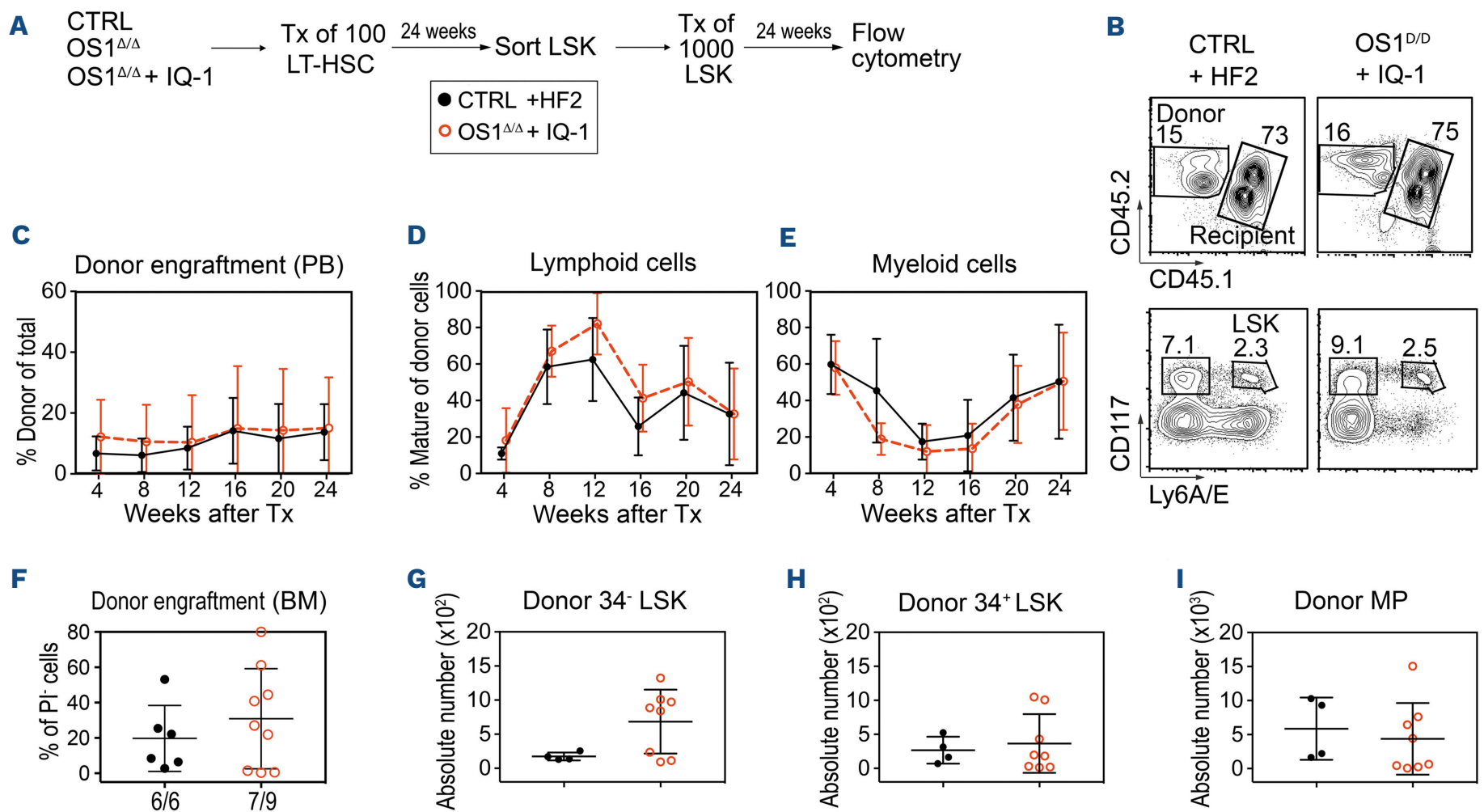

Figure 7. Functionality of long-term hematopoietic stem cells at steady state and after IQ-1 treatment. (A) Experimental design of primary transplantation of IQ-1-treated long-term hematopoietic stem cells (LT-HSC) into lethally irradiated wild-type recipients: 8- to 10-week old OS1[Δ/Δ] mice were injected intraperitoneally for 5 days with IQ-1 (14 μg) or vehicle (HF2). Twenty-four hours after the last treatment 100 LT-HSC were sorted and transplanted into lethally irradiated recipients. (B) Representative flow cytometry plots of the gating strategy of Ly5.2^{+} donor cells or Ly5.1[+]Ly5.2^{+} recipient cells in peripheral blood. (C) Percentage donor cell engraftment in the peripheral blood 4, 8, 12, 16, 20 and 24 weeks after transplantation. (D) Percentage donor engraftment in bone marrow. Absolute numbers of (E) total donor LSK cells; (F) donor CD34^{−} LSK cells; (G) donor CD34^{+} LSK cells; and (H) donor myeloid progenitors of OS1[Δ/Δ] mice (HF2: n=7; IQ-1: n=8) compared to controls (*Sfrp1*^{fl/fl}, HF2: n=9). Each dot represents one animal (D-H). Values are presented as means ± standard deviation. *$P \leq 0.05$ indicates a statistically significant difference determined by analysis of variance, with the Tukey *post-hoc* test. Symbol legends are as shown in (A). CTRL: control; Tx: transplantation; PI: propidium iodide; PB: peripheral blood; BM: bone marrow; MP: myeloid progenitors.

β-catenin are clear, the underlying cellular mechanisms still need to be resolved in detail. In our experiments, the total amount of CBP was not altered, but whether IQ-1 increases the accumulation of β-catenin/CBP co localization is as yet unclear. Since depletion of p300 delays the development of senescence in fibroblasts[18] and specific inhibition of p300 improves stem cell potency,[35,44] reducing nuclear p300 might suffice to improve HSC self-renewal. Our findings that β-catenin is increased in dysfunctional HSC from OS1[Δ/Δ] mice are in line with the observation that high levels of β-catenin induce a functional decline of HSC[45] and increases multilineage differentiation *in vitro* without affecting survival.[46] In addition, considering that SFRP1 is a WNT inhibitor, the association of its deletion and increased canonical WNT signaling would be consistent. To date, the mechanism underlying the association between HSC loss and higher β-catenin levels has not been elucidated. Our findings suggest that increased nuclear localization with a higher probability of β-catenin

binding to p300 may be a possibility. If this is the case, direct or indirect p300 inhibitors such as IQ-1 could promote self-renewal and HSC expansion, similar to embryonic stem cells and induced pluripotent cells.[35] In contrast, this line of reasoning suggests that increasing p300 activity in cells with a high β-catenin level, such as in many cancer stem cells, may help to eradicate these diseases.[47]

Our results indicate that nuclear p300 localization and p300 transcriptional activity in HSC are extrinsically regulated by osteoprogenitors and their progeny in the BM niche. In addition, we provide a rationale and an *in vivo* strategy to normalize p300 localization and restore long-term repopulating HSC activity. Since we applied the PR72/130 inhibitor IQ-1 *in vivo*, it is likely that several different SFRP1-responsive cell types, besides the HSC, were affected. Considering that the BM niche can be regarded as an interwoven ecosystem of different cell-types,[2] *in vivo* IQ-1 treatment does not necessarily act indirectly on

Figure 8. Engraftment of secondary transplanted IQ-1-treated LSK cells. (A) Experimental design of functionality analysis of IQ-1-treated long-term hematopoietic stem cells (LT-HSC) repopulated for 24 weeks in wild-type recipients: 8- to 10-week-old OS1[Δ/Δ] mice were injected intraperitoneally for 5 days with IQ-1 (14 μg) or the vehicle (HF2). Twenty-four hours after the last treatment the LT-HSC were sorted and transplanted into lethally irradiated recipients. Twenty-four weeks after the transplantation, the donor LSK cells were sorted and transplanted into lethally irradiated wild-type recipients. (B) Representative flow cytometry plots of the gating strategy of Ly5.2+ donor cells or Ly5.1+Ly5.2+ recipient cells. (C) Percentage donor cell engraftment in the peripheral blood (PB) up to 24 weeks after the secondary transplant. (D) Percentage lymphoid cells in the PB up to 24 weeks after the secondary transplant. (E) Percentage myeloid cells in the PB up to 24 weeks after secondary transplant. (F) Percentage donor engraftment in bone marrow. Numbers at the top of the graph represent engrafted mice/total mice. (G) Absolute number of donor CD34- LSK cells; (H) donor CD34+ LSK cells; and (I) donor myeloid progenitors of OS1[Δ/Δ] mice (IQ-1: n=8) compared to control mice (*Sfrp1*^{fl/fl}; HF2: n=4). Each dot represents one animal (F-I). Values presented are means ± standard deviation. *P≤0.05 indicates a statistically significant difference determined by an unpaired *t* test. Symbol legends are as shown in (A). CTRL: control; Tx: transplantation; BM: bone marrow; PI: propidium iodide; MP: myeloid progenitors.

HSC through the OS1$^{\Delta/\Delta}$ osteoprogenitors, but may also restore p300 activity in HSC directly. In addition, since IQ-1 interacts with PR72/130 to modulate PP2A activity towards p300 and both p300 and PR72/130 are ubiquitously expressed in the BM of control animals, we cannot exclude that IQ-1 also affects other PP2A-PR72/130 substrates[39,40] or p300 targets which might affect the BM niche or regulate hematopoietic cells in either control or OS1$^{\Delta/\Delta}$ mice.

Our study may be of interest to clinical scientists, since the promoter region of the *SFRP1* gene is hypermethylated in many different cancers and, consequently, SFRP1 expression is reduced.[7] Indeed, reduced SFRP1 expression has been proposed to serve as a prognostic marker.[48] Our findings that OS1$^{\Delta/\Delta}$ mice show reduced HSC activity associated with increased nuclear β-catenin/p300 co localization shows that SFRP1 from osteoprogenitors is critical for regulating the activity of these nuclear factors. We therefore propose that the consequences of *Sfrp1* deficiency, due either to promoter hypermethylation or to gene deletion, could be addressed with inhibitors such as IQ-1 to restore proliferation of quiescent or senescent cells and control differentiation of malignant stem cells.

Disclosures
No conflicts of interest to disclose.

Contributions
FH, CS, RI, and RAJO conceived the study. FH, CS, SRM, BV, TE, TL, RH, RM, HW, RO, RN, and RI were responsible for the methodology. FH, SRM, CS, TL, RH, RM, BV, RN and RI performed the investigations. FH, CS, RI and RAJO wrote the paper. RI and RAJO acquired funds. MR, RN, CP, FB, RR, and RAJO were responsible for the resources. FH, SRM, CS, RI, and RAJO provided supervision.

Data-sharing statement
Original data are available by contacting Robert A.J. Oostendorp (robert.oostendorp@tum.de) or Rouzanna Istvanffy (rouzanna.istvanffy@tum.de). In addition, all RNA-sequencing datasets from the published article are available for download at the European Nucleotide Archive (https://www.ebi.ac.uk/ena) under accession number PRJEB49216.

References

1. Cheng T. Toward 'SMART' stem cells. Gene Ther. 2008;15(2):67-73.
2. Frobel J, Landspersky T, Percin G, et al. The hmatopoietic bone marrow niche ecosystem. Front Cell Dev Biol. 2021;9:705410.
3. Schreck C, Bock F, Grziwok S, Oostendorp RA, Istvanffy R. Regulation of hematopoiesis by activators and inhibitors of Wnt signaling from the niche. Ann N Y Acad Sci. 2014;1310:32-43.
4. Dufourcq P, Descamps B, Tojais NF, et al. Secreted frizzled-related protein-1 enhances mesenchymal stem cell function in angiogenesis and contributes to neovessel maturation. Stem Cells. 2008;26(11):2991-3001.
5. Nakajima H, Ito M, Morikawa Y, et al. Wnt modulators, SFRP-1, and SFRP-2 are expressed in osteoblasts and differentially regulate hematopoietic stem cells. Biochem Biophys Res Commun. 2009;390(1):65-70.
6. Dolgalev I, Tikhonova AN. Connecting the dots: resolving the bone marrow niche heterogeneity. Front Cell Dev Biol. 2021;9:622519.
7. Baharudin R, Tieng FYF, Lee LH, Ab Mutalib NS. Epigenetics of SFRP1: the dual roles in human cancers. Cancers (Basel). 2020;12(2):445.

8. Liang CJ, Wang ZW, Chang YW, et al. SFRPs are biphasic modulators of Wnt-signaling-elicited cancer stem cell properties beyond extracellular control. Cell Rep. 2019;28(6):1511-1525.
9. Fiedler M, Graeb M, Mieszczanek J, et al. An ancient Pygo-dependent Wnt enhanceosome integrated by Chip/LDB-SSDP. Elife. 2015;4:09073.
10. Komiya Y, Habas R. Wnt signal transduction pathways. Organogenesis. 2008;4(2):68-75.
11. Nygren MK, Dosen G, Hystad ME, et al. Wnt3A activates canonical Wnt signalling in acute lymphoblastic leukaemia (ALL) cells and inhibits the proliferation of B-ALL cell lines. Br J Haematol. 2007;136(3):400-413.
12. Patel S, Alam A, Pant R, Chattopadhyay S. Wnt signaling and its significance within the tumor microenvironment: novel therapeutic insights. Front Immunol. 2019;10:2872.
13. Reya T, Clevers H. Wnt signalling in stem cells and cancer. Nature. 2005;434(7035):843-850.
14. Anthony CC, Robbins DJ, Ahmed Y, Lee E. Nuclear regulation of Wnt/beta-catenin signaling: it's a complex situation. Genes (Basel). 2020;11(8):886.

15. Takemaru KI, Moon RT. The transcriptional coactivator CBP interacts with beta-catenin to activate gene expression. J Cell Biol. 2000;149(2):249-254.

16. Teo JL, Ma H, Nguyen C, Lam C, Kahn M. Specific inhibition of CBP/beta-catenin interaction rescues defects in neuronal differentiation caused by a presenilin-1 mutation. Proc Natl Acad Sci U S A. 2005;102(34):12171-12176.

17. Rebel VI, Kung AL, Tanner EA, et al. Distinct roles for CREB-binding protein and p300 in hematopoietic stem cell self-renewal. Proc Natl Acad Sci U S A. 2002;99(23):14789-14794.

18. Sen P, Lan Y, Li CY, et al. Histone acetyltransferase p300 induces de novo super-enhancers to drive cellular senescence. Mol Cell. 2019;73(4):684-698.

19. Man N, Mas G, Karl DL, et al. p300 suppresses the transition of myelodysplastic syndromes to acute myeloid leukemia. JCI Insight. 2021;6(19):138478.

20. Rieger ME, Zhou B, Solomon N, et al. p300/beta-catenin interactions regulate adult progenitor cell differentiation downstream of WNT5a/protein kinase C (PKC). J Biol Chem. 2016;291(12):6569-6582.

21. Renström J, Istvanffy R, Gauthier K, et al. Secreted frizzled-related protein 1 extrinsically regulates cycling activity and maintenance of hematopoietic stem cells. Cell Stem Cell. 2009;5(2):157-167.

22. Jost E, Schmid J, Wilop S, et al. Epigenetic inactivation of secreted frizzled-related proteins in acute myeloid leukaemia. Br J Haematol. 2008;142(5):745-753.

23. Seeliger B, Wilop S, Osieka R, Galm O, Jost E. CpG island methylation patterns in chronic lymphocytic leukemia. Leuk Lymphoma. 2009;50(3):419-426.

24. Wang Y, Krivtsov AV, Sinha AU, et al. The Wnt/beta-catenin pathway is required for the development of leukemia stem cells in AML. Science. 2010;327(5973):1650-1653.

25. Rodda SJ, McMahon AP. Distinct roles for hedgehog and canonical Wnt signaling in specification, differentiation and maintenance of osteoblast progenitors. Development. 2006;133(16):3231-3244.

26. Schreck C, Istvanffy R, Ziegenhain C, et al. Niche WNT5A regulates the actin cytoskeleton during regeneration of hematopoietic stem cells. J Exp Med. 2017;214(1):165-181.

27. Marquez SR, Hettler F, Hausinger R, et al. Secreted factors from mouse embryonic fibroblasts maintain repopulating function of single cultured hematopoietic stem cells. Haematologica. 2021;106(10):2633-2640.

28. Istvanffy R, Vilne B, Schreck C, et al. Stroma-derived connective tissue growth factor maintains cell cycle progression and repopulation activity of hematopoietic stem cells in vitro. Stem Cell Reports. 2015;5(5):702-715.

29. Bodine PV, Zhao W, Kharode YP, et al. The Wnt antagonist secreted frizzled-related protein-1 is a negative regulator of trabecular bone formation in adult mice. Mol Endocrinol. 2004;18(5):1222-1237.

30. Flach J, Bakker ST, Mohrin M, et al. Replication stress is a potent driver of functional decline in ageing haematopoietic stem cells. Nature. 2014;512(7513):198-202.

31. Walter D, Lier A, Geiselhart A, et al. Exit from dormancy provokes DNA-damage-induced attrition in haematopoietic stem cells. Nature. 2015;520(7548):549-552.

32. Wohrer S, Knapp DJ, Copley MR, et al. Distinct stromal cell factor combinations can separately control hematopoietic stem cell survival, proliferation, and self-renewal. Cell Rep. 2014;7(6):1956-1967.

33. Oostendorp RA, Robin C, Steinhoff C, et al. Long-term maintenance of hematopoietic stem cells does not require contact with embryo-derived stromal cells in cocultures. Stem Cells. 2005;23(6):842-851.

34. Buckley SM, Ulloa-Montoya F, Abts D, et al. Maintenance of HSC by Wnt5a secreting AGM-derived stromal cell line. Exp Hematol. 2011;39(1):114-123. e111-115.

35. Miyabayashi T, Teo JL, Yamamoto M, et al. Wnt/beta-catenin/CBP signaling maintains long-term murine embryonic stem cell pluripotency. Proc Natl Acad Sci U S A. 2007;104(13):5668-5673.

36. He K, Xu T, Xu Y, et al. Cancer cells acquire a drug resistant, highly tumorigenic, cancer stem-like phenotype through modulation of the PI3K/Akt/beta-catenin/CBP pathway. Int J Cancer. 2014;134(1):43-54.

37. Schenke-Layland K, Nsair A, Van Handel B, et al. Recapitulation of the embryonic cardiovascular progenitor cell niche. Biomaterials. 2011;32(11):2748-2756.

38. Sasaki T, Kahn M. Inhibition of beta-catenin/p300 interaction proximalizes mouse embryonic lung epithelium. Transl Respir Med. 2014;2:8.

39. Dzulko M, Pons M, Henke A, Schneider G, Kramer OH. The PP2A subunit PR130 is a key regulator of cell development and oncogenic transformation. Biochim Biophys Acta Rev Cancer. 2020;1874(2):188453.

40. Wu CY, Liang Y, Li XF, Song GB. The potential mechanism of PPP2R3A in myocardial cells and its interacting proteins. Eur Rev Med Pharmacol Sci. 2021;25(24):7913-7925.

41. Ugai H, Uchida K, Kawasaki H, Yokoyama KK. The coactivators p300 and CBP have different functions during the differentiation of F9 cells. J Mol Med (Berl). 1999;77(6):481-494.

42. Chan WI, Hannah RL, Dawson MA, et al. The transcriptional coactivator Cbp regulates self-renewal and differentiation in adult hematopoietic stem cells. Mol Cell Biol. 2011;31(24):5046-5060.

43. Zhao Y, Masiello D, McMillian M, et al. CBP/catenin antagonist safely eliminates drug-resistant leukemia-initiating cells. Oncogene. 2016;35(28):3705-3717.

44. Higuchi Y, Nguyen C, Yasuda SY, et al. Specific direct small molecule p300/beta-catenin antagonists maintain stem cell potency. Curr Mol Pharmacol. 2016;9(3):272-279.

45. Luis TC, Naber BA, Roozen PP, et al. Canonical wnt signaling regulates hematopoiesis in a dosage-dependent fashion. Cell Stem Cell. 2011;9(4):345-356.

46. Famili F, Brugman MH, Taskesen E, et al. High levels of canonical Wnt signaling lead to loss of stemness and increased differentiation in hematopoietic stem cells. Stem Cell Reports. 2016;6(5):652-659.

47. Kahn M. Taking the road less traveled - the therapeutic potential of CBP/beta-catenin antagonists. Expert Opin Ther Targets. 2021;25(9):701-719.

48. Rubin JS, Barshishat-Kupper M, Feroze-Merzoug F, Xi ZF. Secreted WNT antagonists as tumor suppressors: pro and con. Front Biosci. 2006;11:2093-2105.